(1:1), 99765-88-5; dibenzyl ketone–DCA (1:8), 99765-89-6; dibenzyl ketone–Dianin's compound (1:45), 99765-90-9; *p*-methylbenzyl benzyl ketone–(β-CD) (1:1.4), 99766-04-8; *p*-methylbenzyl benzyl ketone–DCA (1:8), 99765-91-0; *p*-methylbenzyl benzyl ketone–Dianin's compound (1:22), 99765-92-1; α-methylbenzyl benzyl ketone–(β-CD) (1:1), 99765-93-2; α-methylbenzyl benzyl ketone–DCA (1:8), 99765-94-3; α-methylbenzyl benzyl ketone–Dianin's compound (1:46), 99765-95-4; *p*-methylbenzyl phenylacetate–(β-CD) (1:1), 99765-96-5; *p*-methylbenzyl phenylacetate–DCA (1:8), 99765-97-6; *p*-methylbenzyl phenylacetate–Dianin's compound (1:51), 99765-98-7; benzyl (*p*-methoxyphenyl)acetate–(β-CD) (1:1.3), 99766-05-9; benzyl (*p*-methoxyphenyl)acetate–DCA (1:8), 99765-99-8; benzyl (*p*-methoxyphenyl)acetate–Dianin's compound (1:51), 99766-00-4; *p*-methylbenzyl (*p*-methoxyphenyl)acetate–(β-CD) (1:1.4), 99766-06-0; *p*-methylbenzyl (*p*-methoxyphenyl)acetate–DCA (1:8), 99766-01-5; *p*-methylbenzyl (*p*-methoxyphenyl)acetate–Dianin's compound (1:54), 99766-02-6.

NMR Analysis of Boromycin Sodium Complex and Sodium Desvalinoboromycinate

Todd C. Somers,[1a] James D. White,*[1a] Jung J. Lee,[1b] Paul J. Keller,[1b] Ching-j. Chang,[1c] and Heinz G. Floss*[1b]

Departments of Chemistry, Oregon State University, Corvallis, Oregon 97331, The Ohio State University, Columbus, Ohio 43210, and the Department of Medicinal Chemistry and Pharmacognosy, Purdue University, West Lafayette, Indiana 47907

Received October 25, 1985

Detailed ^1H and ^{13}C NMR assignments were made to the sodium complex of boromycin (**7**) by using two-dimensional chemical shift correlation, NOE difference spectroscopy, and long-range heteronuclear shift correlation (LR-HETCOR). The latter technique was shown to provide a valuable means for assigning ^{13}C signals, including the three carbonyl groups of **7**, by establishing connectivities across quaternary carbons. Similar protocols were used for assigning ^1H NMR signals to the sodium derivative of desvalinoboromycin (**8**). The results of NOE experiments on **7** are consistent with a solution conformation that approximates the tertiary structure of **2**, as revealed by an X-ray crystal structure.

Boromycin (**1**), first isolated from *Streptomyces antibioticus* (Waksman et Woodruff) obtained from an African soil sample,[2] has been encountered in several antibiotic screens, where its activity against gram-positive bacteria, certain fungi, and protozoae has been evaluated.[3] Although early investigation of **1** as a potential coccidiostat has not led to its commercial development,[4] interest in the properties of this ionophore has continued unabated. In particular, the ability of **1** to encapsulate alkali metal cations and transport them across artificial membrane systems has provided a useful tool for studying the mode of action of this antibiotic, which has been shown to reduce the permeability barrier of the cytoplasmic membrane toward potassium ions.[5]

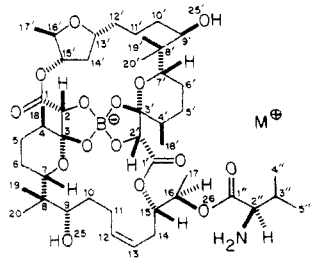

1, M = H
7, M = Na

Structural studies of boromycin by Dunitz, Prelog, et al.[6] revealed that the molecular architecture of this substance is exquisitely designed for its role as an ionophore. An X-ray crystallographic analysis of the rubidium complex **2**, obtained by selective removal of the D-valine residue from **1**, established the complete stereostructure of the macrodiolide, and showed that inward directed oxygen atoms provide an ideal geometry for accommodation of the metal ion. Conversely, the hydrophobic segments of the structure form a nonpolar exterior surface. A similar conformation is observed in the X-ray crystal structure of **3**, in which the borate is absent.[7]

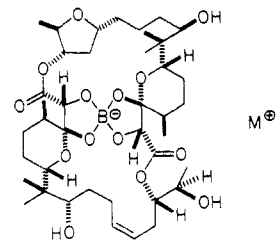

2, M = Rb
8, M = Na

(1) (a) Oregon State University. (b) The Ohio State University. (c) Purdue University.
(2) Hutter, R.; Keller-Schierlein, W.; Knüsel, F.; Prelog, V.; Rodgers, G. C., Jr.; Suter, P.; Vogel, G.; Voser, W.; Zahner, H. *Helv. Chim. Acta* **1967**, *50*, 1533.
(3) Pache, W. In "Antibiotics"; Corcoran, J. W., Hahn, F. E., Eds.; Springer Verlag, New York, 1975; Vol. III, p 585.
(4) Miller, B. M.; Burg, R. W. U.S. Patent 3 864 479, 1975.
(5) Pache, W.; Zähner, H. *Arch. Mikrobiol.* **1969**, *67*, 156.
(6) Dunitz, J. D.; Hawley, D. M.; Miklos, D.; White, D. N. J.; Berlin, Y.; Marusic, R.; Prelog, V. *Helv. Chim. Acta* **1971**, *54*, 1709.
(7) Marsh, W.; Dunitz, J. D.; White, D. M. J. *Helv. Chim. Acta* **1974**, *57*, 10.

0022-3263/86/1951-0464$01.50/0

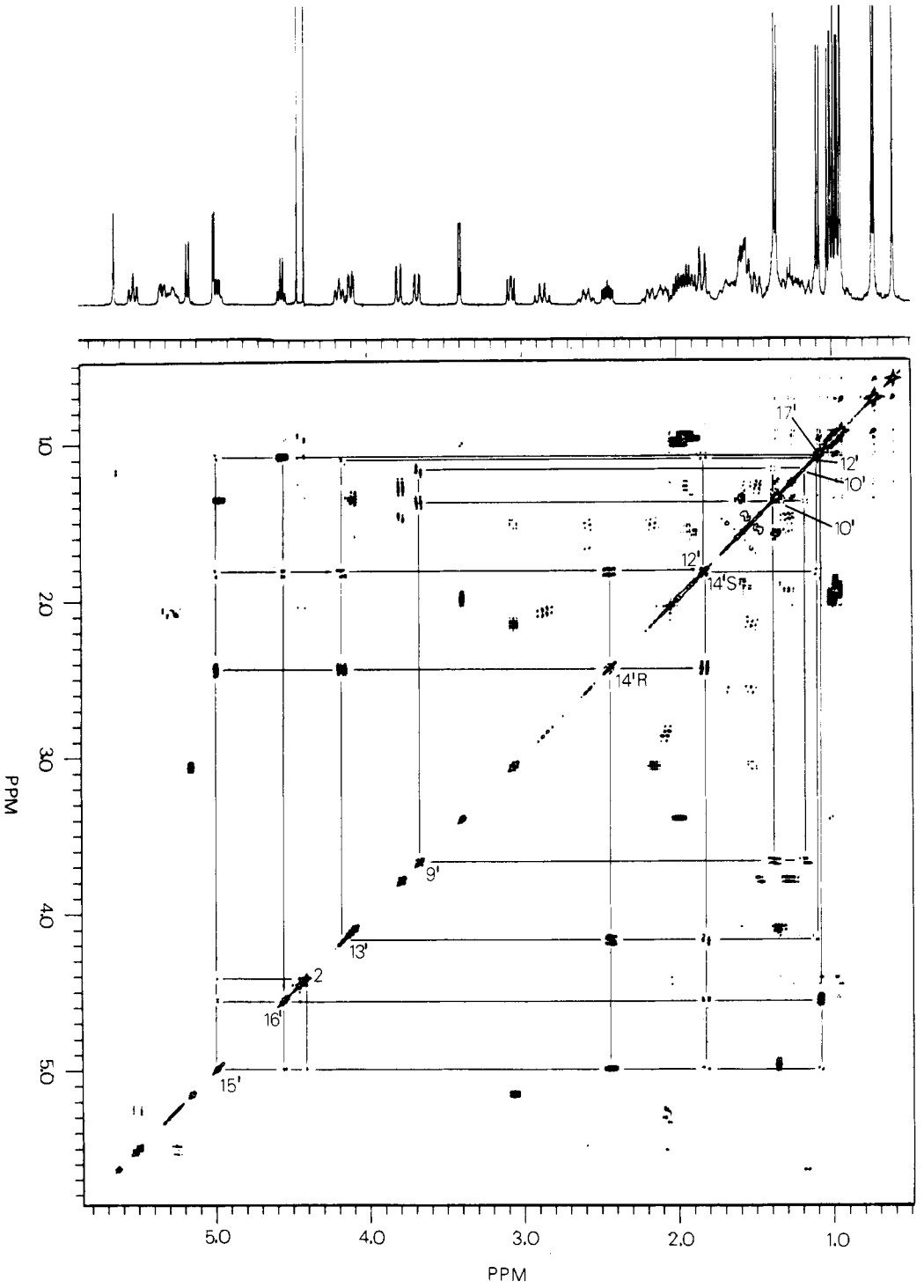

Figure 1. Two-dimensional chemical shift correlated NMR spectrum of the C9′–C17′ segment of 8.

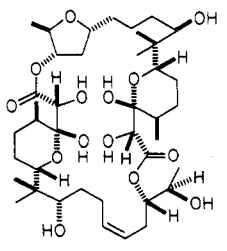

3

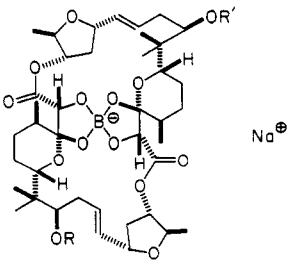

4, R = R′ = H
5, R = H, R′ = Ac
6, R = R′ = Ac

Three closely related antibiotics, aplasmomycins A (**4**), B (**5**), and C (**6**), were isolated more recently from *S. griseus* obtained from a shallow sea sediment.[8] An X-ray

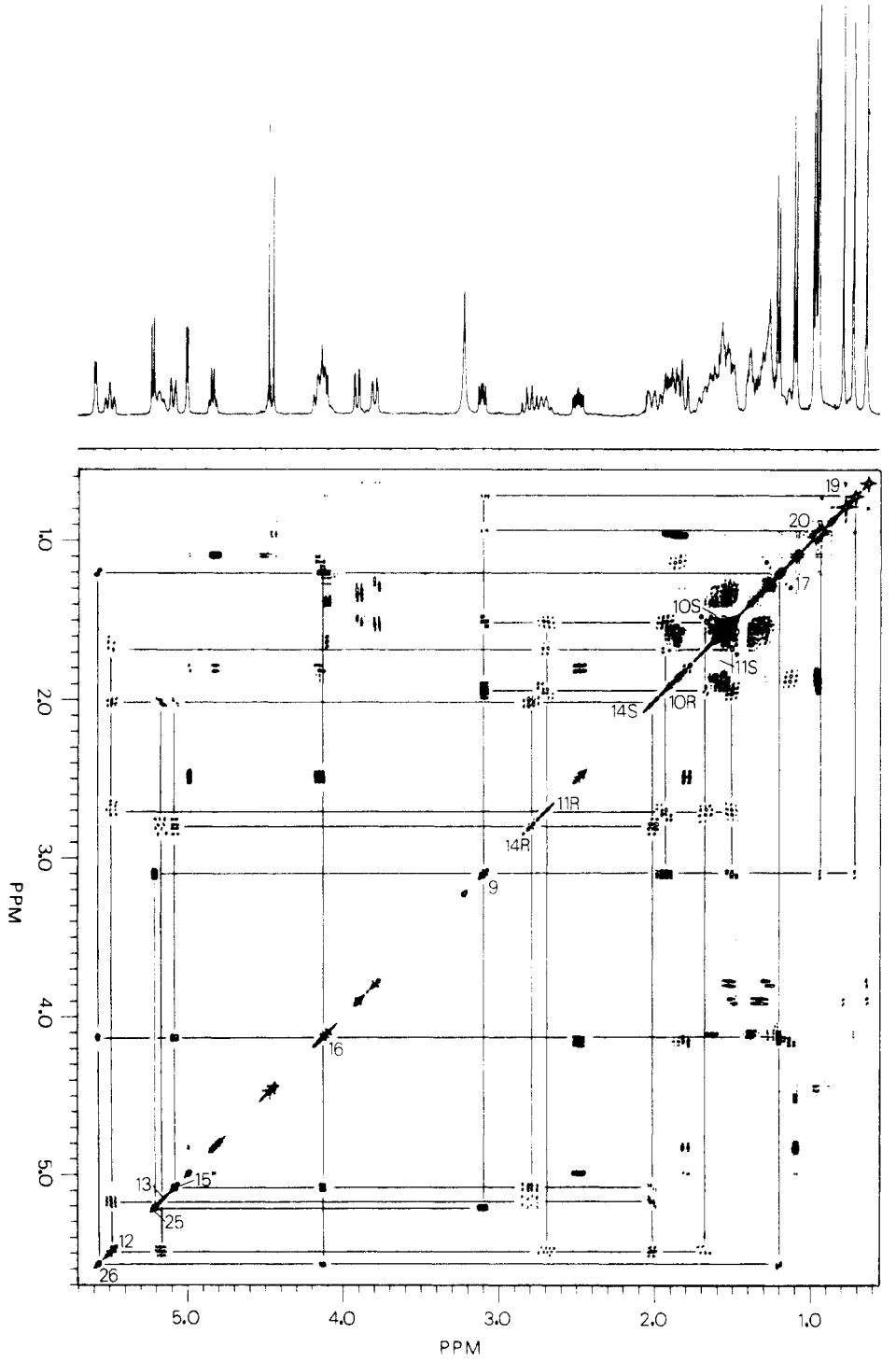

Figure 2. Two-dimensional chemical shift correlated NMR spectrum of the C9–C17 segment of **2**.

crystallographic analysis of the silver salt of **4**, showed that this symmetrical ionophore has many structural features in common with boromycin, including the presence of a borate Böeseken complex and configurational identity with the upper, "northern" half of **1**.[9] Two closely related analogues of **1**, the *N*-formyl and the *N*-acetyl derivatives, have also been isolated.[10]

In the course of synthetic[11] and biosynthetic[12] studies of **1**, it became clear that complete assignment of the ^1H and ^{13}C spectra of **1** would be highly desirable. Although partial attribution of the ^1H resonances in **3**, and the sodium salts of **1** (**7**) and desvalinoboromycin (**8**), had been made previously by spin-decoupling techniques,[13] this

(8) Okazaki, T.; Kitahara, T.; Okami, Y. *J. Antibiot.* **1975**, *28*, 176.
(9) Nakamura, H.; Iitake, Y.; Kitahara, T.; Okazaki, T.; Okami, Y. *J. Antibiot.* **1977**, *30*, 714.
(10) Lee, J. J.; Chen, T. S. S.; Chang, C.-j.; Fenselau, C.; Floss, H. G. *J. Antibiot.* **1985**, *38*, 1444.
(11) White, J. D.; Avery, M. A.; Choudhry, S. C.; Dhingra, O. P.; Kang, M.-c.; Whittle, A. J. *J. Am. Chem. Soc.* **1983**, *105*, 6517. White, J. D.; Choudhry, S. C.; Kang, M.-c. *Tetrahedron Lett.* **1984**, *25*, 3671.
(12) Chen, T. S. S.; Chang, C.-j.; Floss, H. G. *J. Org. Chem.* **1981**, *46*, 2661.
(13) Avery, M. A.; White, J. D.; Arison, B. H. *Tetrahedron Lett.* **1981**, *22*, 3123.

Table I. ^{1}H NMR Assignments to Boromycin Sodium Complex (7) (400.134 MHz)

proton	chem shift, ppm	mult	coupled proton(s) (coupling constant, Hz)
2	4.41	s	
2′	4.45	s	
4	1.90	m	
4′	1.94	m	
5 (2 H)	1.36	m	
5′ (2 H)	1.55	m	
6 (2 H)	1.36, 1.57	m	
6′ (2 H)	1.28, 1.48	m	
7	4.12	dd	6*S* (3.3), 6*R* (9.5)
7′	3.79	dd	6′*S* (1.0), 6′*R* (11.3)
9	3.06	dd	25 (7.5), 10*R* (10.3)
9′	3.67	dd	10′*S* (10.4), 10′*R* (2)
10*R*	2.16	m	
10*S*	1.52	m	
10′ (2 H)	1.18, 1.38	m	
11R	2.58	ddt	12 (10.5), 11*S* (13.5), 10*R* (2.5), 10*S* (10)
11S	1.65	ddd	11*R* (13.5), 12 (<1), 13 (2)
11′ (2 H)	1.24, 1.65	m	
12	5.51	bt	13 (10.5), 11*S* (<1), 11*R* (10.5)
12′ (2 H)	1.10, 1.85	m	
13	5.25	ddt	12 (10.5), 14*R* (11.0), 14*S* (5.5), 11*S* (2)
13′	4.17	bt	14′*R* (9.3), 12′*R* (9.8), 12′*S* (2)
14*R*	2.86	ddd	14*S* (13.5), 15 (11.5), 13 (11.0)
14*S*	2.08	ddd	14*R* (13.5), 13 (5.5), 15 (1)
14′*R*	2.44	ddd	14′*S* (14.1), 15′ (3.8), 13′ (9.3)
14′*S*	1.83	d	14′*R* (14.1)
15	5.32	bd	14*R* (11.5), 16 (1.7), 14*S* (1)
15′	4.99	d	14′*R* (3.8)
16	4.96	dq	17-CH_3 (6.6), 15 (1.7)
16′	4.55	q	17′-CH_3 (6.8)
17 (3 H)	1.36	d	16 (6.6)
17′ (3 H)	1.08	d	16′ (6.8)
18 (3 H)	0.98	d	4 (6.5)
18′ (3 H)	0.95	d	4′ (6.6)
19 (3 H)	0.74	s	
19′ (3 H)	0.60	s	
20 (3 H)	0.94	s	
20′ (3 H)	0.72	s	
2″	3.40	d	3″ (5.4)
3″	1.98	dqq	2″ (5.4), 4″-CH_3, 5″-CH_3 (6.8, 6.8)
4″ (3 H), 5″ (3 H)	1.01, 0.99	d, d	3″ (6.8), 3″ (6.8)
25	5.15	d	9 (7.5)
25′	5.63	s	

Table II. ^{1}H NMR Assignments to Sodium Desvalinoboromycinate (8) (400.134 MHz)

proton	chem shift, ppm	mult	coupled proton(s) (coupling constant, Hz)
2	4.44	s	
2′	4.47	s	
7	4.11	dd	6*S* (4.7), 6*R* (9.7)
7′	3.91	dd	6′*S* (1.7), 6′*R* (11.6)
9	3.11	dd	25 (6.4), 10*R* (10.7), 10*S* (<1)
9′	3.80	dd	10′*S* (12.2), 10′*R* (2.4)
10*R*	1.95	ddt	10*S* (12.9), 11*S* (11.0), 9 (10.7), 11*R* (3.8)
10*S*	1.52	dd	10*R* (12.9), 11*R* (11.0), 9 (<1)
11*R*	2.72	ddt	11*S* (13.2), 12 (11.1), 10*S* (11.0), 10*R* (3.8)
11*S*	1.67	ddd	11*R* (13.2), 10*R* (11.0), 13 (2.6), 12 (<1)
12	5.49	bt	13 (11.1), 11*R* (11.1), 11*S* (<1), 14*S* (<1)
13	5.17	ddt	12 (11.1), 14*R* (11.1), 14*S* (3.6), 11*S* (2.6)
13′	4.17	ddd	12′*R* (11.4), 14′*R* (9.3), 12′*S* (2.3), 14′*S* (<1)
14*R*	2.81	ddd	14*S* (14.0), 15 (11.8), 13 (11.1)
14*S*	2.03	ddd	14*R* (14.0), 13 (3.6), 15 (2.3), 12 (<1)
14′*R*	2.49	ddd	14′*S* (14.6), 13′ (9.3), 15′ (3.8)
14′*S*	1.83	d	14′*R* (14.6), 13′ (<1)
15	5.08	ddd	14*R* (11.8), 16 (2.6), 14*S* (2.3)
15′	5.00	d	14′*R* (3.8)
16	4.14	dq	17 (6.6), 15 (2.6), 26 (4.1)
16′	4.83	q	17′ (6.7)
17	1.20	d	16 (6.6)
17′	1.09	d	16′ (6.7)
18	0.98	d	4 (6.5)
18′	0.96	d	4′ (6.6)
19	0.73	s	
19′	0.64	s	
20	0.95	s	
20′	0.79	s	
25 (9-OH)	5.22	d	9 (6.4)
25′ (9′-OH)	7.30	s	
26 (16-OH)	5.58	d	16 (4.1)

Table III. ^{13}C NMR Assignments to Boromycin Sodium Complex 7 (100.614 MHz)

C	chem shift, ppm	C	chem shift, ppm
1	170.51	3′	105.73
2	78.26	4′	32.77
3	105.13	5′	28.84
4	32.87	6′	25.12
5	25.27	7′	79.89
6	28.33	8′	39.02
7	73.05	9′	76.78
8	39.28	10′	27.95
9	84.56	11′	20.95
10	30.32	12′	35.72
11	26.21	13′	76.89
12	135.05	14′	36.34
13	122.62	15′	79.26
14	26.31	16′	77.75
15	72.91	17′	19.05
16	72.71	18′	16.48
17	16.78	19′	21.33
18	16.68	20′	12.96
19	23.52	1″	172.22
20	19.75	2″	60.80
1′	170.20	3″	33.22
2′	77.25	4″,5″	19.18, 17.32

spectral analysis was inadequate for confident identification of certain synthetic intermediates and for accurate interpretation of precursor incorporation experiments. Consequently, we undertook a comprehensive investigation of the ^{1}H and ^{13}C spectra of boromycin Na complex (7) and the desvalino derivative 8. Assignment of ^{1}H spectral signals, measured at 300 and 400 MHz, was assisted by protium–deuterium exchange, spin-decoupling, two-dimensional chemical shift correlation, and NOE difference spectroscopy. The complete assignment of the ^{13}C spectrum of 7 was made with spin-editing techniques, including long-range ^{1}H–^{13}C heteronuclear shift correlation (LR-HETCOR) spectroscopy.

Results

^{1}H Assignments. Examination of the two-dimensional shift correlated spectrum of 7 permitted a nearly complete assignment of the 7–18, 9–17, 7′–18′, 9′–17′, and 2″–5″ spin systems. These assignments were derived by drawing rectangles between the off-diagonal peaks in the contour plots shown in Figure 1 for the northern portion of 7 (C9′ → C17′) and in Figure 2 for the southern portion (C9–C17) of 8. Although connectivity between protons in the 4–6, 4′–6′, and 10′–12′ segments of 7 was difficult to determine

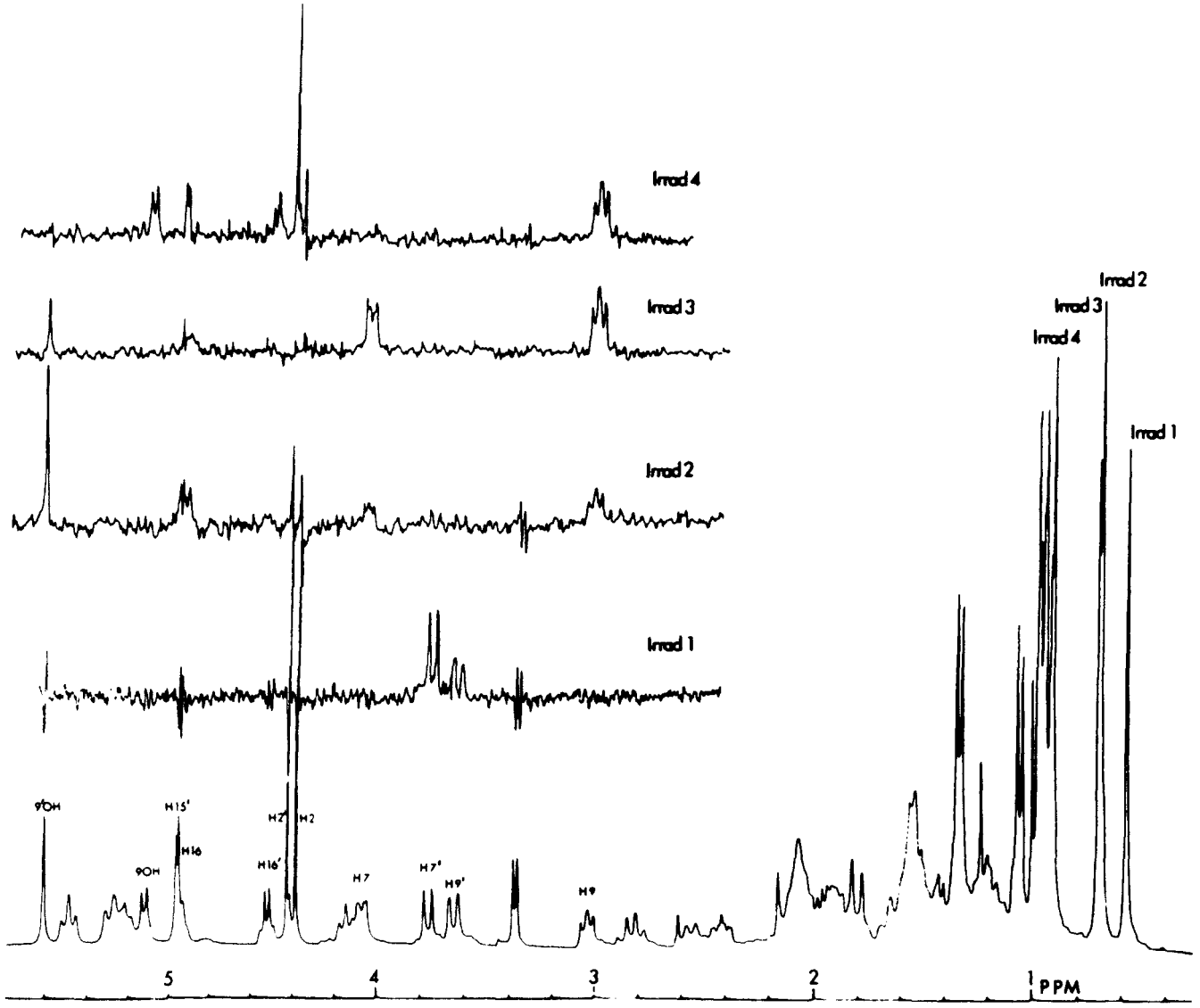

Figure 3. NOE difference spectra of 7.

due to high signal density in the aliphatic region of the spectrum, it was nevertheless possible to identify these protons by examination of the columns and rows of the two-dimensional matrix. For example, columns corresponding to δ 1.18 and 1.38 (H10′ *R,S*) intersected at cross peaks corresponding in each case to δ 1.24 and 1.65 (H11′ *R,S*). The connectivity between H11′ *R,S* and H12′ *R,S*, was established by similar means. Application of the same protocol to the H4–H6 and H4′–H6′ spin systems completed the proton assignments to those segments of the structure of 7 that are separated by quaternary carbons.

It was not possible through this analysis to assign the H2 and H2′ resonances or distinguish the proton signals arising from the tetrahydropyran rings in the northern and southern halves of 7. However, long-range ^1H–^1H couplings were observed in the two-dimensional shift correlated spectrum of 7 (Figure 1) between H15′ and H17′ and between H15′ and H2 which enabled us to tentatively identify the latter proton. This assignment was subsequently confirmed in the course of our ^{13}C spectral analysis of 7 through ^1H–^{13}C correlation spectroscopy. Another feature of interest in the 2D ^1H spectrum of 7 and 8 is the presence of a strong *W* coupling between H14′S and H16′.

The ^1H assignments to 7 given in Table I were completed by using NOE difference spectra. This technique was particularly valuable in distinguishing the two sets of protons in the tetrahydropyran rings through identification of the H7 and H7′ signals as well as the four geminal methyl signals. Irradiation of the methyl singlet at 0.60 ppm in 7 showed NOE effects on signals at 3.79 and 3.67 ppm (Figure 3), identifying these three signals as H19′, H7′, and H9′, respectively. Irradiation at 0.72 and at 0.74 ppm resulted in a major NOE at the 9′-O*H* (H25′) and H16 and at H9 and H7, identifying the two irradiated signals as H20′ and H19, respectively. The folding of 7 brings the C20′ methyl group into proximity with H16 as well as with H25′. The strong NOE on H2′, seen upon irradiation at 0.94 ppm, results from the fact that H18′ resonates close to H20. The latter shows a NOE at H15′ and H16′ as expected from a conformation of 7 that approximates the tertiary structure revealed for the crystalline state. The coupling between H9 and 9-O*H* (H25) suggests that the latter (H25) may form a hydrogen bond to the tetrahydropyran oxygen, which results in deshielding of H7 and shielding of H9. The effect of the $\Delta^{12,13}$ double bond as an alternative explanation for the strong shielding of H9, was ruled out by the observation that hydrogenation of 7 to dihydroboromycin had no effect on the H9 chemical shift. Analogous reasoning using NOE difference spectra (Figure 4) led to the assignments for 8 shown in Table II.

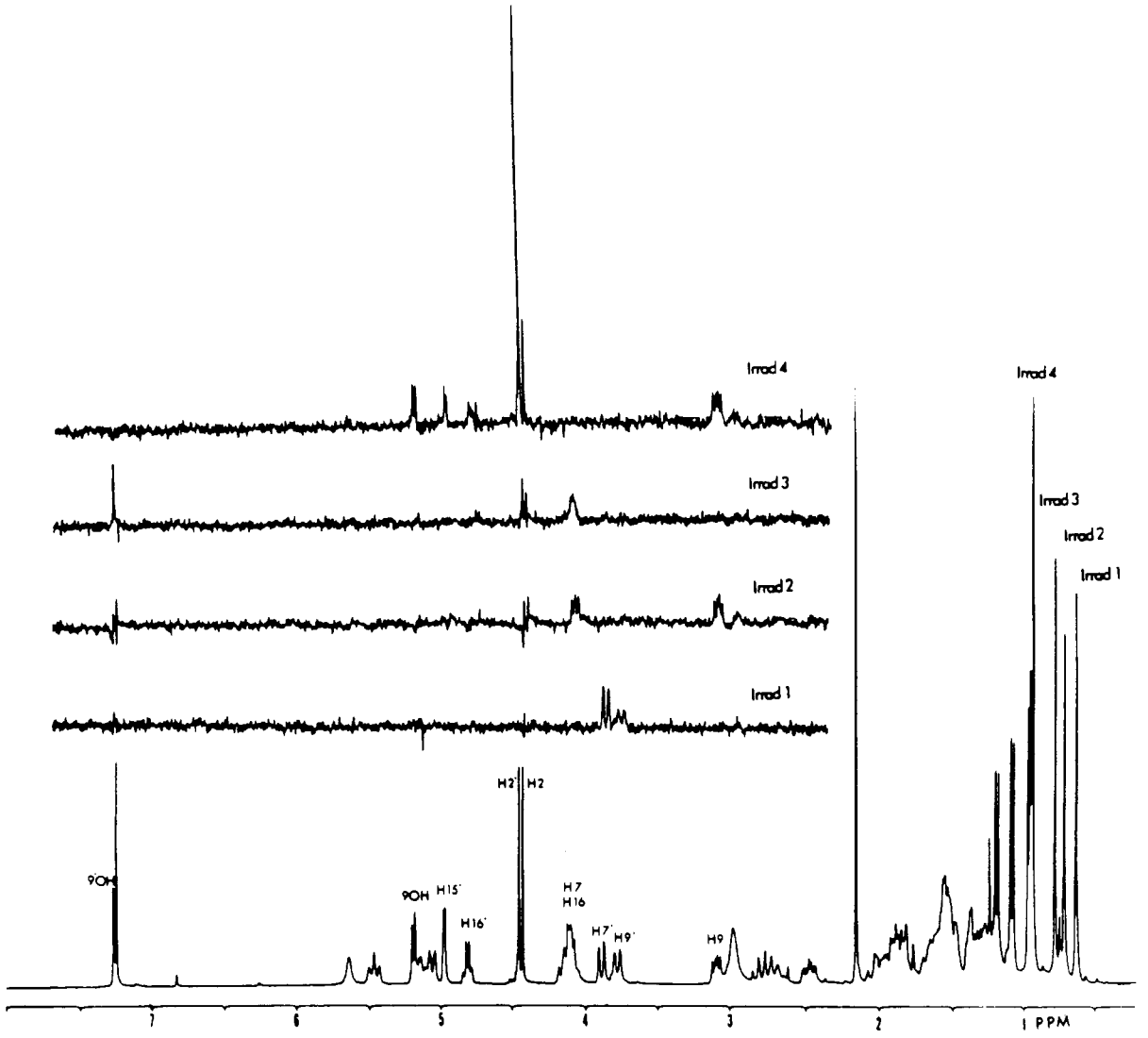

Figure 4. NOE difference spectra of 8.

^{13}C Assignments to Boromycin Sodium Salt (7). A standard DEPT pulse sequence at 100 MHz was employed to delineate the ^{13}C signals due to the 10 methyl carbons, 11 methylene carbons, 17 methine carbons, and 7 quaternary carbons of **7**. With the previously deduced ^{1}H assignments, a heteronuclear ^{1}H-^{13}C shift correlation (HETCOR) (Figure 5) then permitted a detailed analysis of the ^{13}C spectrum. This led to identification of all carbons shown in Table III except the C2,2′ → C8,8′ pairs, the four geminal methyl substituents (C19,19′, C20,20′), and the three carbonyl carbons (C1, C1′, C1″).

In order to complete the carbon assignments to **7**, methods that would provide connectivity across quaternary carbon centers were examined. A widely used pulse sequence for this purpose is the ^{13}C–^{13}C INADEQUATE program.[14] However, this technique has the disadvantage of long acquisition times and a requirement for high sample concentration. In addition, carbonyl carbons are frequently difficult to observe by this procedure due to their long relaxation times. The use of long-range ^{1}H–^{13}C shift correlation[15] appeared to be an attractive alternative, and a pulse program,[16] modified from an earlier sequence,[17] allowed assignment of the remaining 13 carbon atoms. The long-range HETCOR of **7** is displayed in Figure 6, and an expanded version of this correlation in the carbonyl region is shown in Figure 7. Examination of the latter allows identification of the three carbonyl carbons of **7**. Thus, a cross-peak that correlates the proton at δ 3.40 to the carbon resonance at δ 172.22 unambiguously identifies the latter as the valine ester carbonyl (C1″). Also, the carbon resonance at δ 170.51 shows coupling to H15′ at δ 4.99 as well as a proton at δ 4.41, thereby permitting assignment of not only the C1 carbonyl and H2 proton, but the C2 methine carbon as well. The third carbonyl (C1′) at δ 170.20 shows an analogous correlation to H2′ and H15.

In order to assign unambiguously the ^{1}H and ^{13}C resonances to the two tetrahydropyran rings of **7**, it was necessary to establish connectivity between C7 and C9 and between C7′ and C9′. Again, the long-range HETCOR sequence conveniently solved this problem by revealing a coupling of C9 with two proton signals at δ 0.74 and 0.94, which were clearly the position 19 and 20 geminal methyl

(14) Bax, A.; Freeman, R.; Frenkiel, T. A.; Levitt, M. H. *J. Magn. Reson.* **1981**, *43*, 478.
(15) Seto, H.; Furihata, K.; Otake, N.; Itoh, Y.; Takaheshi, S.; Haneishi, T.; Ohuchi, M. *Tetrahedron Lett.* **1984**, *25*, 337.
(16) Sato, Y.; Geckle, M.; Gould, S. J. *Tetrahedron Lett.* **1985**, *26*, 4019.
(17) Bleich, H.; Gould, S. J.; Pitner, P.; Wilden, J. *J. Magn. Reson.* **1984**, *56*, 575.

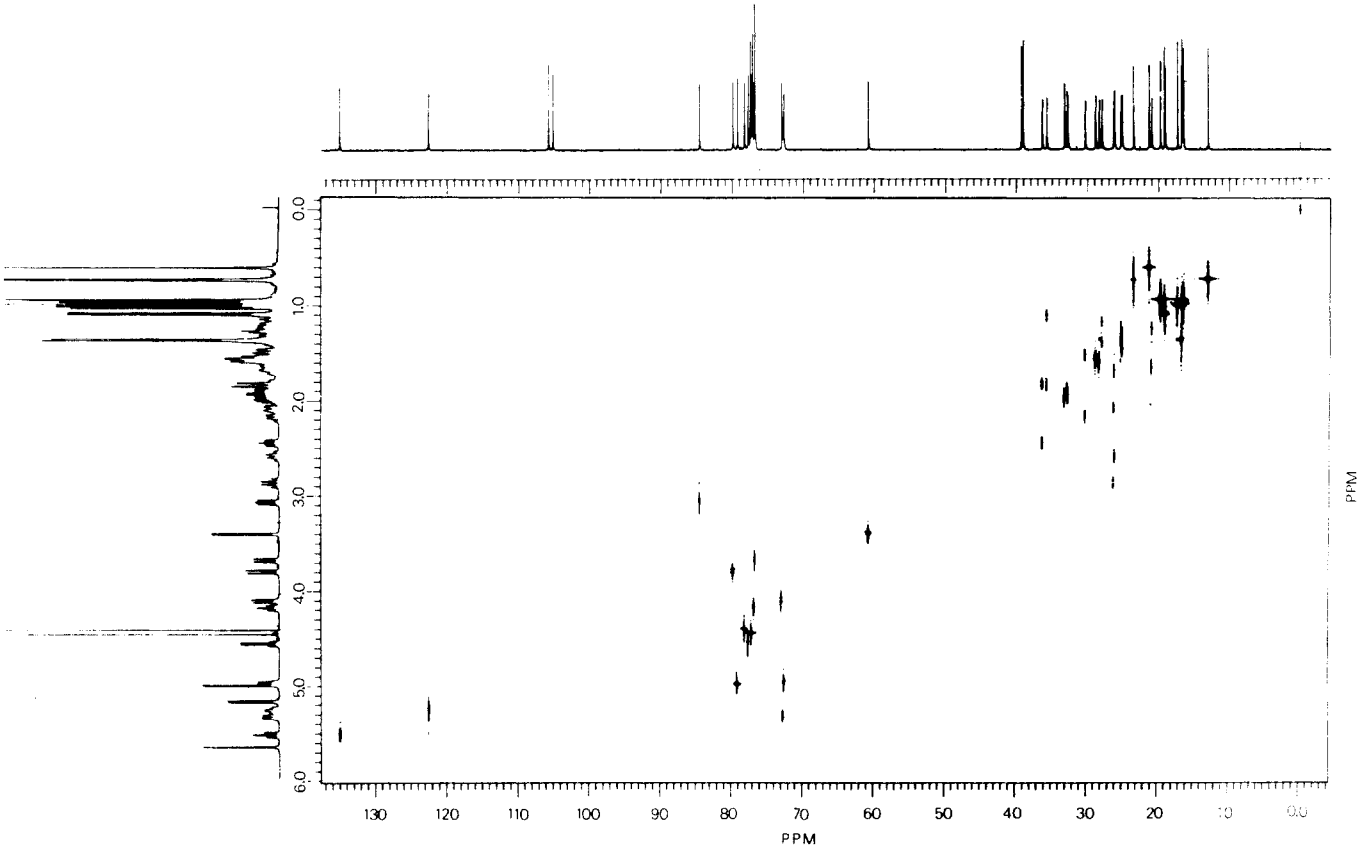

Figure 5. Heteronuclear $^{1}H-^{13}C$ chemical shift correlated spectrum of **7**.

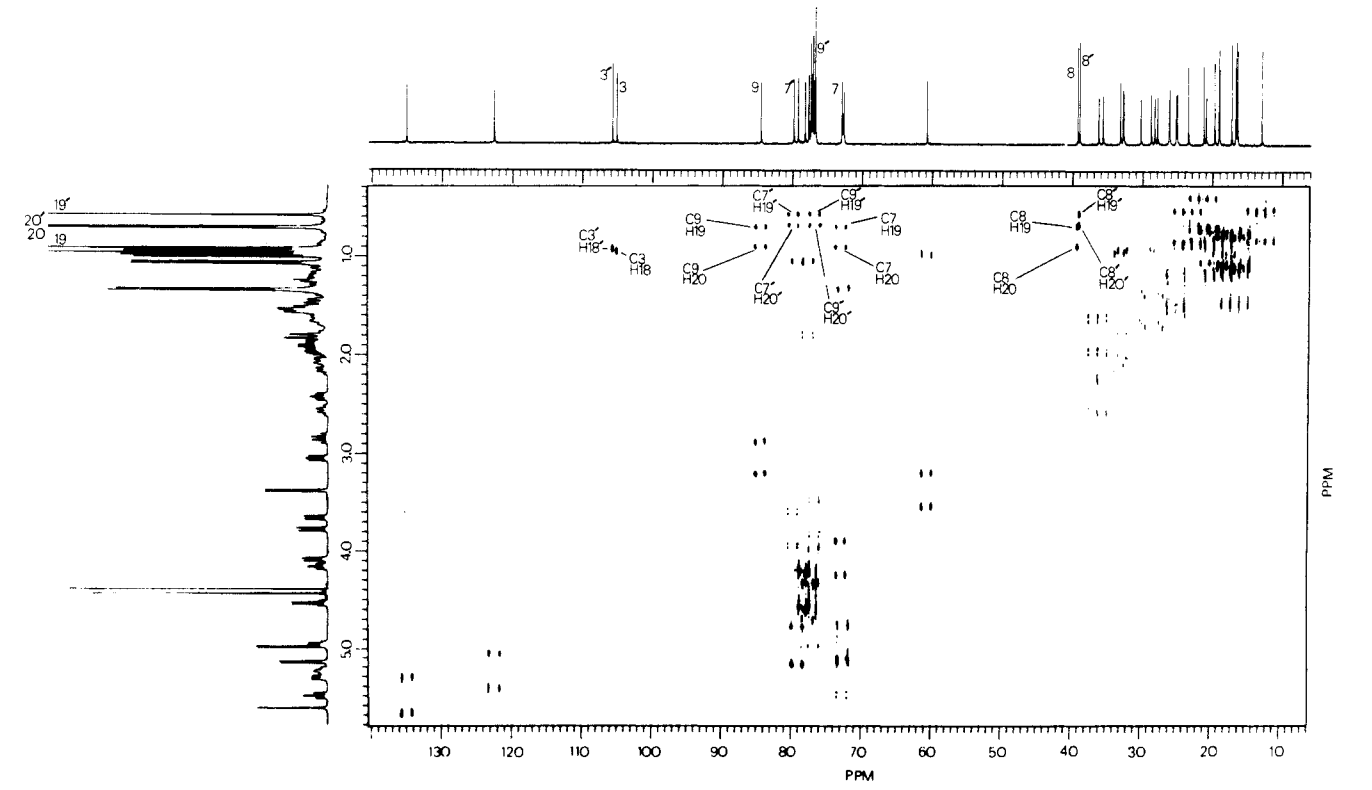

Figure 6. Long-range heteronuclear $^{1}H-^{13}C$ chemical shift correlated spectrum of **7**.

substituents. These same methyl resonances were coupled to C7 and C8 at δ 73.05 and 39.28, respectively, thus providing the logic needed for complete assignment to this segment. The C7′–C9′ spin system was analyzed in similar fashion, leading to the analogous carbon assignments in the northern half of **7**.

Finally, the long-range $^{1}H-^{13}C$ shift correlation disclosed the identity of the quaternary carbons at C3 and C3′. A

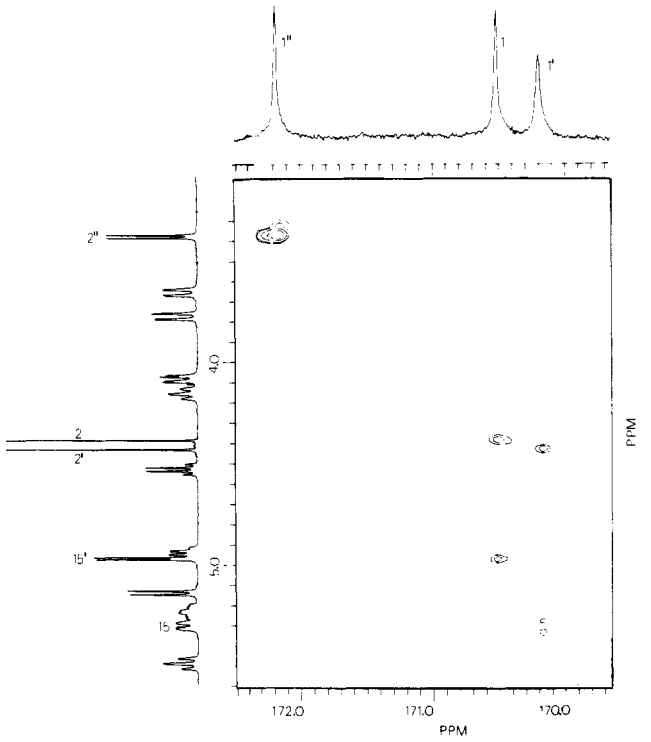

Figure 7. Carbonyl region of the long-range heteronuclear ^1H–^{13}C chemical shift correlated spectrum of **7**.

strong correlation between the signal at δ 105.13 and the C18 methyl protons at δ 0.98 established the C3 resonance, while a parallel correlation between C3′ (δ 105.73) and the C18′ methyl group (δ 0.95) afforded the last piece of data to complete a full carbon spectral analysis of **7**.

Experimental Section

The boromycin sodium complex (**7**) used in this study was obtained from Merck and Co. Approximately 80 mg of the complex was dissolved in 0.5 mL of $CDCl_3$, containing 0.1% Me_4Si as an internal standard, resulting in a concentration of 0.18 M. A solution of 15 mg of sodium desvalinoboromycinate (**8**)[6] in 0.5 mL of $CDCl_3$, containing 0.1% Me_4Si as an internal standard resulted in a concentration of 0.038 M. The solutions were transferred to 5-mm NMR tubes and used for all subsequent 2D NMR studies.

NOE difference spectra for **7** and **8** were measured with sample concentrations of 0.045 and 0.049 M, respectively, on a Bruker AM 300 spectrometer. A presaturation time of 3 s was used with an effective decoupler power of $\gamma_H Hz/2\pi$ = 16.78 Hz. Data sets of 16K covering a spectral width of 3500 Hz were acquired. A 1.0-Hz line broadening was applied to the data prior to Fourier transformation.

All two-dimensional spectra of **7** and **8** were recorded at 297 K with a Bruker AM 400 spectrometer equipped with an Aspect 3000 computer operating in the Fourier transform mode with quadrature detection. Standard Bruker pulse programs (version 840301.1) were used unless otherwise noted.

The two-dimensional ^1H–^1H shift correlated (COSY-45) data for **7** were acquired at a sweep width of 2500 Hz (4096 data points) in the F2 domain; 1024 spectra (16 scans each) were accumulated with 0.400 ms increments across the interval 3μs to 409.603 ms. A 1-s recycle delay was inserted between scans to allow spin relaxation. The digital resolution was 1.221 Hz/pt in both dimensions after zero-filling in F1. Resolution enhancement was accomplished by application of a $\pi/2$ shifted sinebell window function to F1 and F2 prior to Fourier transformation. The COSY-45 data for **8** were acquired and processed under identical conditions except that a 2577-Hz sweep width was used in the F2 domain.

The heteronuclear ^1H–^{13}C shift correlated (HETCOR) experiment for **7** was performed with a 14 285 Hz (4096 data point) spectral width in the F2 (^{13}C) dimension and a ±1231 Hz (512 data point) window in the F1(^1H) domain; 512 individual spectra (32 transients each) were acquired at an incremental delay of 0.203 ms across the interval 3 μs to 103.939 ms. Two dummy scans were used between files with a 1-s recycle delay between scans. Zero-filling afforded digital resolution in the F1 and F2 dimensions of 2.405 and 6.975 Hz/pt, respectively. A Gauss–Lorentz resolution enhancement of 0.300 with a −1.000 line broadening was applied to both domains before Fourier transformation.

The long-range heteronuclear shift correlated (LR-HETCOR) spectral data for **7** were acquired with sweep widths of 17 241 Hz (4096 data points) in the F2(^{13}C) domain and ±1400 Hz (256 data points) in the F1(^1H) dimension. Zero-filling afforded digital resolution in F1 and F2 of 5.469 and 8.419 Hz/pt, respectively; 256 spectra were accumulated of 128 transients each, with an incremental delay of 0.3571 ms over the interval 3 μs to 91.4206 ms. Two dummy scans were used between files with a 1-s recycle delay between scans. Resolution enhancement was achieved by application of a Gauss–Lorentz multiplication of 0.500 and a line broadening of −1.000 in F2 and a $\pi/4$-shifted sinebell in the F1 domain prior to transformation.

Acknowledgment. We are indebted to Drs. Ralph Hirschmann and John Hannah, Merck and Co., for a sample of boromycin. Financial support was provided by the National Institutes of Health through Grants AI10964 (to J.D.W.) and AI20264 (to H.G.F.). Funds for the purchase of a Bruker AM 400 spectrometer were provided by the National Science Foundation through Grant CHE-8216190 and by the M. J. Murdock Charitable Trust, Vancouver, WA.

Registry No. **7**, 55222-09-8; **8**, 80373-43-9.